Kinematic Calibration and Geometrical Parameter Identification for Robots

Jean-Michel Renders, Eric Rossignol, Marc Becquet, and Raymond Hanus

Abstract—**This paper presents a new technique for the calibration of robots based on a maximum likelihood approach for the identification of geometrical errors. A new experimental setup is presented for measurement of the end-effector position errors. The errors of position and orientation of the measuring device are included in the algorithm and identified. Tests have been carried out on a robot with six degrees of freedom (DOF). Tests show that this technique can reduce the mean error distance by a factor of more than 15. Finally, compensation algorithms are presented, based on the improved knowledge of the geometrical model.**

I. Problem Statement

ONE of the most important breakthroughs in robot technology is the off-line programming process in CAD system that makes possible the general design and layout of a robotic cell and also the robot task simulation. The most important output of this simulation is a task file that can be downloaded into the robot control system to perform the desired motions. Much work is undertaken nowadays to make off-line programming an attractive tool that will enlarge the spectrum of robot applications in manufacturing processes.

The major problem is the difference between the notional geometry of a robot, based on the robot design specifications, and the real geometry of the same robots affected by manufacturing tolerances, mounting errors during robot link assembly, and kinematic model simplifications in the control unit. Notional models used are simple and are based on several assumptions, such as parallelism or orthogonality of the axes of the joints. Differences between nominal and real kinematic models also rise from nongeometrical errors e.g., link-and-joint flexibility, backlash, gear runout, and the like.

Robot kinematic calibration consists of identifying a more accurate geometrical relationship between the joint encoder readings and the actual position of the end-effector; then the robot positioning software is changed according to this relationship identified. Kinematic calibration involves four steps: modeling, measurement, identification, and correction.

The purpose of this paper is to present a new calibration method including a new algorithm to identify differences between the nominal and real robot geometry and an original experimental setup to apply the method in a real case. The results of our method can be included in a larger design process of robots similar to the work presented in Jiang *et al.* [6].

Robot position error models have been widely studied. A linearized geometrical error model has been established by Veitschegger and Wu [18]; it was used for *a priori* accuracy analysis but not for identification and calibration purposes. The same thing can be said about the work of Menq and Borm [20]; they studied the statistical properties of the position error of the end-effector employing probabilistic characterization of the unknown geometrical parameters; but their paper does not deal with identification, measurement, and calibration problems.

Hollerbach and Bennett [3] and An *et al.* [4] used Veitschegger's linearized error model for geometrical parameter identification and gave some experimental results. However, they did not include position and orientation errors of the measuring device in the modeling process, and, using the common least-squares method for identification, they did not take into account *a priori* information (sensor accuracy, manufacturing tolerances, etc.). Moreover, no significant experimental results were obtained, because of insufficient accuracy of the measuring device.

Roth *et al.* [21] give an overview of robot calibration discussing modeling, measurement, identification, and correction issues, but no mathematical developments or experimental results are presented.

Whitney *et al.* [13] use a model including nongeometrical errors and a least squares numerical search algorithm on theodolite measurements. The error model is completely nonlinear and, unfortunately, the definition of geometrical parameters to be identified (six for each link) is rather unusual and related to the measuring instruments.

Judd and Knasinski [14] consider mainly nongeometrical errors (gear train errors, joint and link flexibility, etc.) and proposes error models that can be used for identification with a common least squares procedure.

The contribution of the work in the area of kinematic calibration is composed of two main points. First, experimental results in arm calibration using a new kind of motion tracking system are reported; unlike other measurement methods already proposed in the literature (see [1], [4], [9], [12], [13], [16]), this system is simple and economically attractive while providing sufficient accuracy for calibration purpose. Second, an algorithm for estimating geometrical parameter errors is presented, taking into account the following characteristics: sensor accuracy, resolver resolution,

Manuscript received September 26, 1989; revised January 30, 1991. The portions of this work performed at the Arc Robotique were supported by the S.P.P.S., a service of the Prime Minister.

J.-M. Renders, E. Rossignol, and M. Bequet are with the Arc Robotique, Université Libre de Bruxelles, Brussels, Belgium.

R. Hanus is with the Laboratoire d'Automatique, Université Libre de Bruxelles, Brussels, Belgium.

IEEE Log Number 9101641.

backlash in transmission units, manufacturing tolerances, and, finally, position and orientation errors of the measuring device. These limits are used for building a global error model and a maximum likelihood estimator. Such an approach, although yielding identification results with a sounder theoretical justification, has not been adopted in previous work.

The paper is organized as follows. In Section II, we introduce the definition of the geometrical parameters; the effects of nongeometrical errors and the measuring device limitations are discussed; the differential modeling with the maximum likelihood estimator and its properties are described; finally, we establish the global model, including position errors of the measuring device. Section III presents two experiments carried out on a robot with six degrees of freedom (DOF). Different ways to use the improved kinematic model obtained after identification are described in Section IV. Finally, concluding remarks appear in Section V.

II. Error Model

In this section we will build up the global model for error identification. This model depends on the choice of parameters used to describe the robot geometry and on the possible consideration of non-geometrical errors; the error model is written in a linearized form so that it can be directly exploited in the identification process. A maximum likelihood estimator is built, taking into account possible backlash in transmission units, measuring device limits and manufacturing tolerances.

A. Geometrical Parameters

A classical choice for the geometrical parameters used to describe the robot geometry is the Denavit–Hartenberg parameters (θ_i, d_i, a_i, and α_i). But it is well known that, with this set of four parameters, small geometrical errors do not lead to small variations of the parameters. For example, if two successive rotational joints are parallel, the common normal defining the distance between those two axes may be arbitrarily located. If they are slightly nonparallel, this distance may greatly vary in magnitude and position. For this reason, it can be convenient to use an extra parameter (Veitschegger and Wu [18]): this extra parameter defines a rotation of a frame (i) to a new frame (i') resulting from nonexactly parallel rotational axis; around the y_i axis it is called the link twist β_i (see Fig. 1). Without this link twist, the nonparallelism must be compensated for by artificial modification to the values of the length a_i and the offset d_i of the link, even if they were initially correct.

This twist angle β_i is useful only for successive nominally parallel rotational joint axis. In this case, it is substituted for the joint offset error d_i, so that we are allowed to fix the dependent translation d_i and to consider that it is error free. In other cases it is set to zero. Nominal values of those geometrical parameters can be different from the real ones in the robot system because manufacturing tolerances and assembly tolerances affect the kinematic model of the robot; moreover, the electrical zeroes of the joint encoders do not generally coincide with the mechanical zeroes of the joints themselves.

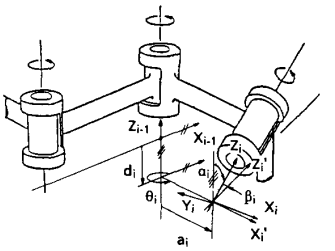

Fig. 1. Definition of the Denavit–Hartenberg parameters, including the link twist β_i.

In Section II-D and subsequent sections, we develop an identification algorithm to find the errors for the geometrical parameters.

B. Nongeometrical Errors

As depicted in Section II-A, geometrical parameters can be affected by errors on their nominal values. But other error sources are present in a robot structure. We will call them nongeometrical errors sources. Among these, the error sources that have the most significant effect on accuracy are joint flexibility, link flexibility, gear transmission error, backlash in gear transmission, and temperature effect. According to results presented in the literature, flexibility in joints and in links is responsible for 8%–10% of the position and orientation errors of the end effector (see [11], [13], [14], [17]).

Link flexibility is usually less than joint flexibility: bellows 5% (see [17]). Joint flexibility errors could be substantially reduced by mounting the joint encoders directly on the joint after the transmission units, instead of mounting them on the motor shaft.

Gear transmission errors are mainly due to runout and orientation errors: runout appears when the center of rotation does not lie at the center of the pitch circle of the gear, whereas orientation error appears when the shafts of a ring gear and a pinion gear are not parallel. Judd and Knasinski [14] have proposed a gearing error model combining these effects with six extra parameters for each joint.

Backlash is probably one of the most difficult error source to identify. Fortunately, its contribution to the global error is only from 0.5%–1.0%. Identification of backlash is difficult mostly because the gears may be anywhere inside the backlash dead zone. From this point of view, we do not follow Whitney *et al*'s statement [13] that gears are always on one extreme of the dead zone. We justify our point of view by the fact that dry friction may be important in robot mechanism and that a static equilibrium of the mechanism can be found inside the dead zone and not only on one extreme of that zone.

Temperature effect expands the robot mechanical structure. Given the materials used for robot links and their thermal expansion coefficient, the error due to temperature effects is responsible for 0.1% of the total error. This means that for present purpose it can be ignored, and measurements do not

have to be carried out in a constant temperature environment. All nongeometrical errors are responsible for about 10% of the total error. In the following sections we will restrict our analysis to geometrical errors to simplify the equations but without any loss of generality.

C. Measuring Device Limitations

The measurement of a three-dimensional (3D) trajectory with high accuracy, large bandwidth, and large displacement is still difficult to achieve. To illustrate this statement we will briefly discuss five major means to measure 3D trajectories of the end effector.

String-operated potentiometric transducers may be used to compute the position of a specific point of the manipulator on which three strings are connected. This system can be accurate enough and large displacements are allowed, but its bandwidth is limited and the system reliability must be carefully considered. Such a system is presented in [9] with experimental results.

Laser measurement systems are highly accurate, their bandwidths are sufficient, and large displacements are allowed, but currently they can be used only for linear motions. Various research is in progress to develop 3D measurements laser systems, but motion speed seems to be limited (see [16]).

Ultrasonic 3D measurements systems are available on the market. Along each Cartesian axis the resolution reaches 0.1 mm and sampling rate is about 50 Hz. An important disadvantage of this system is the sensitivity of sound speed in the air to temperature and humidity. Thus calibration will be required several times during measurements. Because the sonic source is fixed to the moving object, problems can occur with reflections of the sonic wave on the moving object structure, in this case on the robot structure. Microphones can detect those reflections and thus give a wrong information on the source position. The reader can find results of the use of ultrasonic systems and extensive comments thereon in [15].

Infrared 3D measurement systems have also been available for a few years. These are based on a stereoscopic analysis by two cameras of the location of an infrared light-emitting diode (LED) fixed to the end effector. Three LED's can be used and switched on and off in sequence so that three fixed points of the end effector can be located. In this way, the absolute position and orientation of a Cartesian frame fixed on the end effector can be known. Resolution is about $\frac{1}{4000}$ of full scale, which depends on the relative location of the two cameras. This system needs accurate calibration and is also sensitive to reflections. Such a system was used by Hollerbach and Bennett [3], and An *et al.* [4]. The low resolution directly influences the accuracy which, in the judgement of the researchers concerned, was simply not good enough for kinematic calibration. New developments have been carried out [12] for infrared 3D measurement systems to bring accuracy up to the level of laser-based systems.

Another possible technique of measurement consists in using theodolites and stereo triangulation. This technique was used in [11], [13] and [14]. Despite the fact that theodolites provide very good accuracy and allow measurements over a wide area of robot workspace, a major drawback is that measurements can only be performed statically and not during the robot motion. It is time consuming and fatiguing, although automatic tracking theodolites exist; moreover, theodolites only measure angles, not lengths, which can cause some problems (need of reference length in particular).

From this review of 3D measurement systems we conclude that it is very difficult to achieve this task mainly for technical reasons but also for economic ones. In fact, it is not necessary to make complete measurement of the end-effector position for calibration purposes. Instead, several equivalent incompletely specified position measurements are sufficient. For example, constraining a point of the end-effector to remain on a given plane or sphere corresponds to one condition. This is realized when a robot tactile sensor is brought into contact with a flat plane or surface of a fixture (cube or spherical surfaces). Another technique consists of constraining the position of lines attached to the end-effector: one possibility is to use an optical sensor in the robot hand and to bring it into a position at which the optical beam just gets broken due to contact with the surface of a fixture [12].

For all those reasons we have focused our work on straight line motion analysis. The measuring device shown in Fig. 2 was designed taking into account the fact that a straight line motion is easier to track than a general curve and that such a device will be less expensive (see [18]). The device consists of a magnetostrictive sensor for the longitudinal displacement (along the straight line) and of two magnetic transducers for the two transversal displacements (in a plane perpendicular to the straight line). The range of the longitudinal sensor is 1000 mm and accuracy 0.1 mm. The range of each magnetic transducer is 15 mm and the resolution is 0.6 μm.

Considering the complete setup for measurement, including data acquisition device and measuring device, the accuracy in each direction is about 0.1 mm. The procedure requires minimal human involvement because it is sufficient to program a straight-line motion that follows roughly the axis of the measurement device; automatic data acquisition can be performed easily once the robot carries out with its movement. Complete information for one line can therefore be gathered in a few seconds. These are two sources of limitations in the use of the measuring device: accuracy and position and orientation of the measuring device with respect to the robot base frame. The second source of limitations is ignored in most papers dealing with this subject. In fact, it is possible to consider the errors of position and orientation of the measuring device by adding extra parameters in the global model (see Section II-H). It is nothing more than an extra link between the robot base (conventional) and the absolute zero of the measuring device. A total of six extra parameters are required for each measuring line: three for the position error of the measuring device and three for the orientation error of the measuring device. Of course, these extra parameters will require additional measures to allow their identification.

Another important aspect is that one straight line is not enough to identify the complete set of parameters. For each

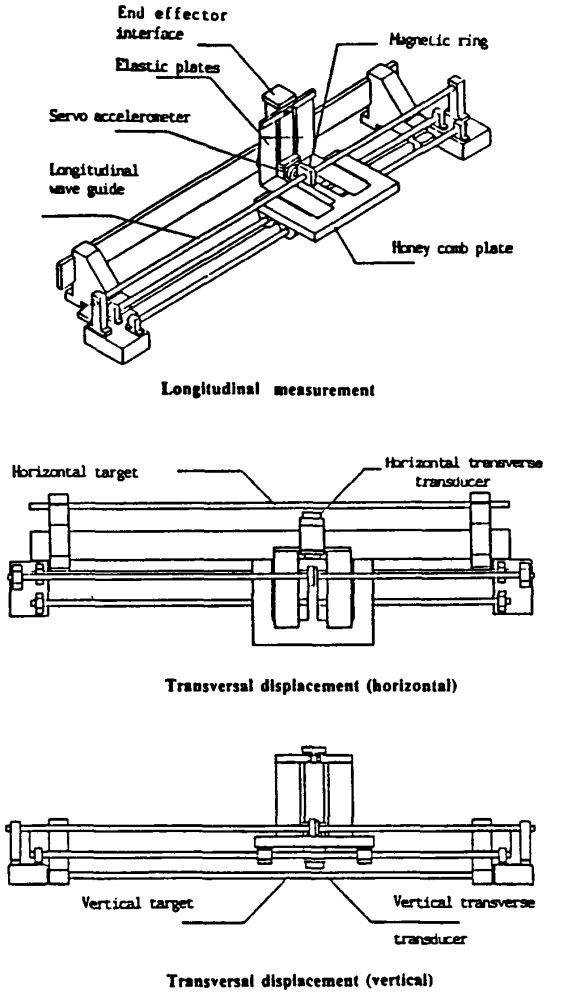

Fig. 2. Description of the measuring device: linear motion tracking system with one magnetostrictive sensor (longitudinal displacement) and two magnetic transducers (transversal displacement).

new line, we will add six unknown parameters corresponding to the measuring device position and orientation errors. Some insights for choosing the measuring lines are given in Section III-G.

D. Differential Modeling

The direct geometrical model gives the end-effector position and orientation vector x as a function of the geometrical parameters in a general form given by

$$x = f(\theta, \alpha, a, d, \beta) \tag{1}$$

where θ, α, a, d, and β are R^n vectors for an n-joint robot. This relation is strongly nonlinear in the geometrical parameters. In order to identify them we choose to linearize this model around an initial estimate $\hat{\theta}$, $\hat{\alpha}$, $\hat{a}$, $\hat{d}$, $\hat{\beta}$ (nominal parameters) of the real parameters θ, α, a, d, β. Because two successive parallel axis of rotation are initially supposed to be parallel, we choose $\hat{\beta}_i = 0$ for each link. A differential model can be obtained as follows:

$$\Delta x = J_\theta \Delta\theta + J_\alpha \Delta\alpha + J_a \Delta a + J_d \Delta d + J_\beta \Delta\beta \tag{2}$$

where $\Delta\theta$ is the systematic error vector on the angles θ_i (joint encoder offsets), $\Delta\alpha$, Δa, Δd, and $\Delta\beta$, error vectors on the torsion angles α_i, on the lengths a_i, on the offsets d_i, on the twist angles β_i, respectively (all these vectors belong to R^n); and

$$J_\theta = \frac{\partial f}{\partial \theta}, \qquad J_\alpha = \frac{\partial f}{\partial \alpha}, \text{etc.}$$

Each of these Jacobian matrices is the sensitivity matrix of the end-effector position and orientation with respect to geometrical parameter variation. These matrices are computed using the initial estimates $\hat{\theta}$, $\hat{\alpha}$, $\hat{a}$, $\hat{d}$, $\hat{\beta}$ for the geometrical parameters. Their computation can be performed by using a symbolic program as presented in [10] or by evaluating each columns by simple vector relationships [4] such as

$$\{J_{\theta i}\} = \begin{Bmatrix} [{}^0_{i-1}R]\left(\{\mathbf{1}z_{i-1}\} x \{{}^{i-1}P_N\}\right) \\ [{}^0_{i-1}R]\{\mathbf{1}z_{i-1}\} \end{Bmatrix}$$

where $[\,]$, $\{\,\}$, and x respectively denote matrix, vector, and cross-product; $[{}^0_{i-1}R]$ is the rotation matrix from frame $(i-1)$ to the base frame (o); $\{{}^{i-1}P_N\}$ is the end-effector position vector expressed in frame $(i-1)$; and $\{\mathbf{1}z_{i-1}\} = \{0, 0, 1\}^t$; and similar expressions are used for the other Jacobian matrices.

At this stage, computation of the Jacobian matrices is useful for *a priori* analysis: when we know statistical properties of the geometrical parameters (which are related to manufacturing and assembly tolerances), we can establish the statistical properties of the position error of the end-effector, to characterize the distribution of the position errors over the working space to determine working areas with less significant errors, and to find the direction of motion in which the smallest position errors will most probably occur [20].

Knowing $\hat{\theta}$, $\hat{\alpha}$, $\hat{a}$, $\hat{d}$, $\hat{\beta}$, and computing $\Delta\theta$, $\Delta\alpha$, Δa, Δd, $\Delta\beta$, we can establish a new estimate of the real parameters θ^*, α^*, a^*, d^*, β^* given by:

$$\theta^* = \hat{\theta} + \Delta\theta$$
$$\alpha^* = \hat{\alpha} + \Delta\alpha, \text{etc.}$$

Since this is essentially a nonlinear estimation problem, a new geometrical parameter error vector can be recalculated after updating the geometrical parameters, using the same maximum likelihood estimator (see next section), in an iterative way until the error components fall below some minimum value and the parameters converge to some stable values.

E. Maximum Likelihood Estimator

The model obtained with (2) that we will write in short

$$\Delta x = J \text{th}\, \Delta\theta$$

is an ideal differential error model without considering input and output noises. We now consider the case where only the position error is modeled ($\Delta x \epsilon R^3$). Here, $\Delta\theta$ represents the

complete geometrical parameter error vector with n components where n is the total number of geometrical parameters to be identified. Our first assumption (A1) will consist of considering that this model is valid over the complete robot workspace. This implies that we do not take into account nongeometrical errors (backlash, flexibility, etc.). The measures we have to make are the end-effector position error vector Δx_i the ith point of measure ϵR^3 and the joint variable vector given by the resolvers $q_i \epsilon R^6$, for a robot with six rotational joints. Those two vectors are affected by noise, respectively:

$$\delta x_i \epsilon R^3$$
$$\delta q_i \epsilon R^6.$$

Thus, the measured error vector is given by $\Delta x_i^m = \Delta x_i + \delta x_i$, where the superscript m indicates measured quantities.

Our second assumption (A2) is that δx_i and δq_i are Gaussian white-noise vectors, with independent components with zero mean and with constant covariance matrices, respectively:

$$S_x = \begin{bmatrix} \sigma_{x1}^2 & 0 & 0 \\ 0 & \sigma_{x2}^2 & 0 \\ 0 & 0 & \sigma_{x3}^2 \end{bmatrix}.$$

The values of σ_{xi}^2 are obtained from the knowledge of the measuring device accuracy:

$$S_q = \begin{bmatrix} \sigma_{q1}^2 & & 0 \\ & \ddots & \\ 0 & & \sigma_{q6}^2 \end{bmatrix}.$$

The values of σ_{qi}^2 are obtained from the knowledge of resolver accuracy and backlash in transmission units (assuming that backlash can be modeled by a Gaussian white noise). Following those assumptions, we can define a linearized noisy model as follows:

$$(\Delta x_i^m - \delta x_i) = J_i \Delta\theta + J_{2,i} \delta q_i \tag{3}$$

where $\Delta\theta$ is a short form for errors on geometrical parameters ϵR^n, J_i is a short form for the global Jacobian matrix $\epsilon R^{3\times n}$, function of the nominal parameters, and $J_{2,i}$ is the manipulator Jacobian $\epsilon R^{3\times 6}$, function of the nominal parameters.

Our third assumption (A3) is that the linearized noisy model is also valid over the complete robot workspace. The fourth assumption (A4) that we will consider is to assume that the random vector $\Delta\theta \epsilon R^n$ follows an *a priori* Gaussian distribution with independent components, zero mean, and a covariance matrix

$$S_\theta = \begin{bmatrix} \sigma_{\theta 1}^2 & & 0 \\ & \ddots & \\ 0 & & \sigma_{\theta n}^2 \end{bmatrix}.$$

The values of $\sigma_{\theta i}^2$ are obtained from the knowledge of robot link manufacturing tolerances and assembly tolerances. Finally, we will assume that δx_i, $\Delta\theta$, and δq_i are mutually independent random variables (A5).

Following the Bayesian approach, using the *a priori* distribution of $\Delta\theta$, we can form the likelihood function [19]:

$$L = \text{cst} \exp\left\{ -\tfrac{1}{2}\left(\sum_{i=1}^{N} \delta x_i^t M_x \delta x_i + \sum_{i=1}^{N} \delta q_i^t M_q \delta q_i + \Delta\theta^t M_\theta \Delta\theta \right) \right\} \tag{4}$$

with

$$M_x = S_x^{-1}, \qquad M_q = S_q^{-1}, \qquad M_\theta = S_\theta^{-1} \tag{5}$$

and N is the number of measurement points. To find the maximum likelihood estimator we have to maximize L or to minimise the following cost function:

$$L' = \tfrac{1}{2} \sum_{i=1}^{N} \delta x_i^t M_x \delta x_i + \tfrac{1}{2} \sum_{i=1}^{N} \delta q_i^t M_q \delta q_i + \tfrac{1}{2} \Delta\theta^t M_\theta \Delta\theta. \tag{6}$$

To the function L' we have to add the equations of constraints given by the linearized noisy model using the Lagrange multipliers. The global cost function over the N measures is given by

$$L = \tfrac{1}{2} \sum_{i=1}^{N} \delta x_i^t M_x \delta x_i + \tfrac{1}{2} \sum_{i=1}^{N} \delta q_i^t M_q \delta q_i + \tfrac{1}{2} \Delta\theta^t M_\theta \Delta\theta + \sum_{i=1}^{N} \lambda_i^t \left[(\Delta x_i^m - \delta x_i) - J_i \Delta\theta - J_{2i} \delta q_i \right]. \tag{7}$$

The minimization equations lead to

$$\frac{\partial L}{\partial \Delta\theta} = 0 \Rightarrow M_\theta \hat{\Delta\theta} - \sum_{i=1}^{N} J_i^t \lambda_i = 0 \tag{8}$$

$$\frac{\partial L}{\partial \delta x_i} = 0 \Rightarrow M_x \delta x_i - \lambda_i = 0 \tag{9}$$

$$\frac{\partial L}{\partial \delta q_i} = 0 \Rightarrow M_q \delta q_i - J_{2,i}^t \lambda_i = 0 \tag{10}$$

$$\frac{\partial L}{\partial \lambda_i} = 0 \Rightarrow \Delta x_i^m - \delta x_i = J_i \Delta\theta + J_{2,i} \delta q_i \tag{11}$$

Equations (9) and (10) yield

$$M_q \delta q_i = J_{2,i}^t M_x \delta x_i \rightarrow \delta q_i = M_q^{-1} J_{2,i}^t M_x \delta x_i$$

with (11):

$$\Delta x_i^m - J_i \Delta\theta = \delta x_i + J_{2,i} M_q^{-1} J_{2,i}^t M_x \delta x_i.$$

Thus,

$$\delta x_i = \left(I + J_{2,i} M_q^{-1} J_{2,i}^t M_x \right)^{-1} \left(\Delta x_i^m - J_i \hat{\Delta\theta} \right)$$

or, in short,

$$\delta x_i = A_i \left(\Delta x_i^m - J_i \hat{\Delta\theta} \right)$$

with A_i a 3×3 matrix.

Equations (8) and (9) yield

$$M_\theta \widehat{\Delta\theta} = \sum_{i=1}^{N} J_i^t M_x \delta x_i = \sum_{i=1}^{N} J_i^t M_x A_i \left(\Delta x_i^m - J_i \widehat{\Delta\theta}\right)$$

which leads to

$$\left(M_\theta + \sum_{i=1}^{N} J_i^t M_x A_i J_i\right)\widehat{\Delta\theta} = \sum_{i=1}^{N} J_i^t M_x A_i \Delta x_i^m.$$

If we call $M_x A_i = C_i$, which is a symmetric matrix, equal to

$$C_i = \left(M_x^{-1} + J_{2,i} M_q^{-1} J_{2,i}^t\right)^{-1}$$

we then have

$$\left(M_\theta + \sum_{i=1}^{N} J_i^t C_i J_i\right)\widehat{\Delta\theta} = \sum_{i=1}^{N} J_i^t C_i \Delta x_i^m$$

and finally

$$\widehat{\Delta\theta} = \left(M_\theta + \sum_{i=1}^{N} J_i^t C_i J_i\right)^{-1} \sum_{i=1}^{N} J_i^t C_i \Delta x_i^m. \quad (12)$$

F. Recursive Computation

As we will see hereafter, it is possible to compute the "least squares solution" corresponding to (12) in a recursive way [19]. Let $\widehat{\Delta\theta}(N-1)$ be the estimate of the solution after $(N-1)$ measures.

$$\widehat{\Delta\theta}(N-1) = \left(M_\theta + \sum_{i=1}^{N-1} J_i^t C_i J_i\right)^{-1} \sum_{i=1}^{N-1} J_i^t C_i \Delta x_i^m. \quad (13)$$

By taking

$$P(N-1) = \left(M_\theta + \sum_{i=1}^{N-1} J_i^t C_i J_i\right)^{-1} \quad (14)$$

and noting that $P(0) = M_\theta^{-1}$, we have

$$\widehat{\Delta\theta}(N-1) = P(N-1) \cdot \sum_{i=1}^{N-1} J_i^t C_i \Delta x_i^m. \quad (15)$$

The estimate of the solution after N measures is now given by

$$\widehat{\Delta\theta}(N) = P(N) \sum_{i=1}^{N} J_i^t C_i \Delta x_i^m \quad (16)$$

Equation (14) leads to

$$P(N)^{-1} = P(N-1)^{-1} + J_N^t C_N J_N. \quad (17)$$

Using the matrix inversion lemma [19]

$$\left[A + BCD\right]^{-1} = A^{-1} - A^{-1}B \cdot \left[DA^{-1}B + C^{-1}\right]^{-1} DA^{-1}$$

it can be shown that

$$P(N) = P(N-1) - P(N-1) \cdot J_N^t \left(C_N^{-1} + J_N P(N-1) J_N^t\right)^{-1} \cdot J_N P(N-1). \quad (18)$$

Equation (18) is used to compute recursively the matrix $P(N)$.

Equations (13) and (17) yield

$$\sum_{i=1}^{N-1} J_i^t C_i \Delta x_i^m = P(N-1)^{-1} \widehat{\Delta\theta}(N-1) = P(N)^{-1} \widehat{\Delta\theta}(N-1) - J_N^t C_N J_n \widehat{\Delta\theta}(N-1). \quad (19)$$

Eqs. (16) and (19) give

$$\widehat{\Delta\theta}(N) = P(N) \cdot \left(\sum_{i=1}^{N-1} J_i^t C_i \Delta x_i^m - J_N^t C_N \Delta x_N^m\right) = P(N)\left(P(N)^{-1} \widehat{\Delta\theta}(N-1) - J_N^t C_N J_N \widehat{\Delta\theta}(N-1) + J_N^t C_N \Delta x_N^m\right).$$

We thus arrive at the algorithm

$$\widehat{\Delta\theta}(N) = \widehat{\Delta\theta}(N-1) = P(N) J_N^t C_N \left[\Delta x_N^m - J_N \widehat{\Delta\theta}(N-1)\right]. \quad (20)$$

Equation (2) can be used to compute recursively the estimate of the solution as a function of the previous estimate $\widehat{\Delta\theta}(N-1)$, the matrix $P(N)$, and the prediction error $(\Delta x_N^m - J_N \widehat{\Delta\theta}(N-1))$.

G. Properties of the Recursive Estimator

Multiplying (3) by $J_i^t C_i$ and summing over all measures, we can obtain the following result:

$$\left(M_\theta + \sum_{i=1}^{N} J_i^t C_i J_i\right)\Delta\theta = \sum_{i=1}^{N} J_i^t C_i \Delta x_i^m - \sum_{i=1}^{N} J_i^t C_i \delta x_i - \sum_{i=1}^{N} J_i^t C_i J_{2,i} \delta q + M_\theta \Delta\theta. \quad (21)$$

We will now define

$$\tilde{\theta}_N = \widehat{\Delta\theta}(N) - \Delta\theta \quad (22a)$$

the *a posteriori* estimation error, and

$$\tilde{\theta}_o = \widehat{\Delta\theta}(0) - \Delta\theta = 0 - \Delta\theta \quad (22b)$$

the *a priori* estimation error.

Subtracting (21) from (12), we obtain

$$\left(M_\theta + \sum_{i=1}^{N} J_i^t C_i J_i\right)\tilde{\theta}_N = \sum_{i=1}^{N} J_i^t C_i \delta x_i + \sum_{i=1}^{N} J_i^t C_i J_{2,i} \delta q_i + M_\theta \tilde{\theta}_o. \quad (23)$$

Equation (23) leads to:

$$\tilde{\theta}_N = P(N) \cdot \left(\sum_{i=1}^{N} J_i^t C_i \delta x_i + \sum_{i=1}^{N} J_i^t C_i J_{2,1} \delta q_i + M_\theta \tilde{\theta}_o\right). \quad (24)$$

Following assumptions (A2), (A4), and (A5),

$$\langle \delta x_i \rangle = 0$$
$$\langle \delta q_i \rangle = 0$$
$$\langle \tilde{\theta}_o \rangle = 0$$

(where the symbol "$\langle\rangle$" means mathematical expectation) we have $\langle \hat{\theta}_N \rangle = 0$, which demonstrates that the estimator is unbiased.

We can also show that the variance of the *a posteriori* estimation error is equal to $P(N)$:

$$\begin{aligned}\langle \tilde{\theta}_N \tilde{\theta}_N^t \rangle &= P(N)\big[\textstyle\sum J_i^t C_i M_x^{-1} C_i^t J_i \\ &\quad + \textstyle\sum J_i^t C_i J_{2,i} M_q^{-1} J_{2,i}^t C_i^t J_i \\ &\quad + M_\theta M_\theta^{-1} M_\theta \big] P(N) \qquad (25)\\ \langle \tilde{\theta}_N \tilde{\theta}_N^t \rangle &= P(N)\big[\textstyle\sum J_i^t C_i \big(M_x^{-1} \\ &\quad + J_{2,i} M_q^{-1} J_{2,i}^t \big) C_i^t J_i + M_\theta \big] P(N) \\ &= P(N)\big[\textstyle\sum J_i^t C_i J_i + M_\theta \big] P(N) \\ &= P(N) P(N)^{-1} P(N) = P(N). \qquad (26)\end{aligned}$$

H. The Global Model

The global model is obtained by adding to the model represented by (7) the effect of position and orientation errors with respect to the robot base frame of the measuring device. The contribution to the error on the robot end-effector position for the ith measure due to a position error Δx_j^d, Δy_j^d, Δz_j^d, and orientation error $\Delta \phi_{xj}^d$, $\Delta \phi_{yj}^d$, and $\Delta \phi_{zj}^d$ of the jth measuring line is obtained by

$$e_i = J_{ij}^d \Delta x_j^d \qquad (27)$$

where Δx_j^d is a short form for Δx_j^d, Δy_j^d, Δz_j^d, $\Delta \phi_{xj}^d$, $\Delta \phi_{yj}^d$, $\Delta \phi_{zj}^d (\epsilon R^6)$ (superscript d indicates values related to the measuring *d*evice and J_{ij}^d is the measuring device Jacobian matrix for the ith measure on the jth measuring line ($\epsilon R^{3\times 6}$). The matrix J_{ij}^d is given by

$$J_{ij}^d = \left(I_3, - \hat{P}_{j,i} \right) \qquad (28)$$

where I_3 is the unit matrix ($\epsilon R^{3\times 3}$), $\hat{P}_{j,i}$ is the skew symmetric matrix ($\epsilon R^{3\times 3}$) corresponding to the cross-product $P_{j,i} \times \Delta\phi$, with $P_{j,i}$ the coordinates of the ith measurement point on the jth line with respect to the measuring device reference frame: $\hat{P}_{j,i} \Delta\phi \triangleq P_{j,i} \times \Delta\phi$. Thus, (3) becomes for the global model

$$\left(\Delta x_i^m - \delta x_i \right) = J_i \Delta\theta + J_{2,i} \delta q_i + J_{ij}^d \Delta x_j^d$$

if point i is located on the jth measuring line.

Consequently, we can choose an extended parameter vector $\Delta\theta$, including Δx_j^d for all j, and an extended Jacobian matrix J_i, including J_{ij}^d (which is nonzero only if the ith measurement point belongs to the jth measuring line). All our results and developments are therefore also valid for the global model.

I. Comparison with Other Identification Techniques

Our maximum likelihood estimator is a generalized least squares identification algorithm, including a probabilistic characterization of measurement noise and of unknown robot parameters (*a priori* distributions). The common least squares algorithm, which has always been adopted in previous calibration works (see [1], [4], [5], [14] is a particular case of the maximum likelihood estimator where

$S_x = I_3$ (3×3 identity matrix),
$S_q = 0$ (joint encoders readings are assumed error free), and
$S_\theta = P(0) = P_0 I_n$ (P_0 is an arbitrary large number).

In (18) and (20), the matrix C_N is then the identity matrix and these equations become identical to the recursive least squares formulas [19, p. 20]. From this point of view, we can conclude that our method is a better approach because, in a Bayesian framework, it takes into account *a priori* information on the output observations ($S_x \neq I_3$), *a priori* information on the input readings ($S_q \neq 0$), and *a priori* information on the parameter vector (S_θ), which is related to the initial condition of the covariance matrix $P(0)$ (Bayesian interpretation).

It is well known that using all available prior information gives better results in convergence and stability [19, pp. 299–303]. For example, if initial values θ_0 are known with good precision, large value of $P(0)$ would cause abrupt transients and a more difficult convergence. On the other hand, when $P(0)$ is too small (too much confidence given to the erroneous initial values), the convergence can be very slow. This suggest that, for a given finite number of measured data, the identification results will be more accurate when *a priori* information is employed. These considerations will be illustrated by an example on a real case in Section III.

III. Application

A. Study Case

The kinematic calibration algorithm was applied to one of our robots, developed in our laboratory, which has six degrees of freedom (see Fig. 3). This robot is controlled by a Siemens RCM-SIROTEC control unit. In this system, most of the geometrical parameters are factory programmed and can not be modified by the user. The consequences of this fact will be investigated subsequently.

B. Nominal Values

Table I gives the nominal values of the geometrical parameters.

C. Covariance Matrices

The following values based on measuring device accuracy, resolver resolution, and manufacturing tolerances were used

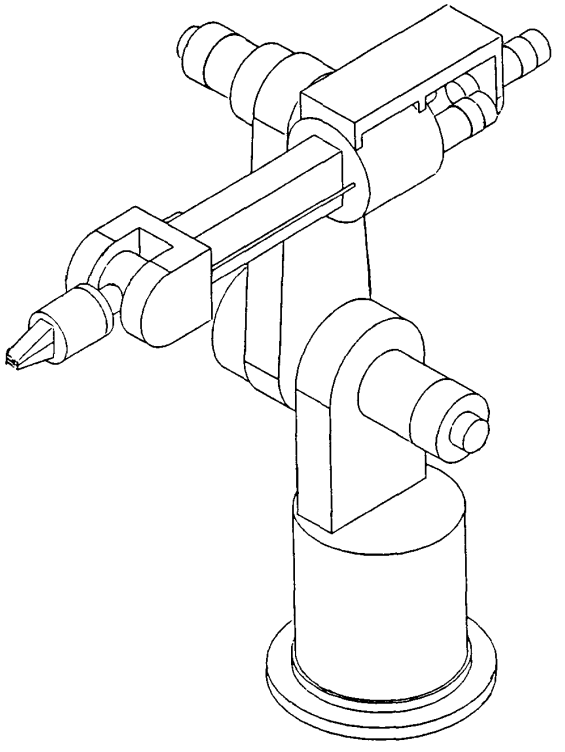

Fig. 3. ULB manipulator (6 DOF).

TABLE I
NOMINAL VALUES OF GEOMETRICAL PARAMETERS
(ANGLES IN RADIANS, LENGTHS IN METERS)

i	α_i	a_i	d_i	θ_i
1	$-(\frac{\pi}{2})$	0	0	θ_1
2	0	0.350	0	θ_2
3	$(\frac{\pi}{2})$	0	0	θ_3
4	$-(\frac{\pi}{2})$	0	0.350	θ_4
5	$(\frac{\pi}{2})$	0	0	θ_5
6	0	0	0.1	θ_6

in the different covariance matrices:

$$S_x = 10^{-9}\begin{bmatrix} 3.84 & 0 & 0 \\ 0 & 10 & 0 \\ 0 & 0 & 3.84 \end{bmatrix}[\mathrm{m}^2]$$

$$S_q = 10^{-9}\begin{bmatrix} 21 & 0 & 0 & 0 & 0 \\ 0 & 21 & 0 & 0 & 0 \\ 0 & 0 & 21 & 0 & 0 \\ 0 & 0 & 0 & 1.31 & 0 \\ 0 & 0 & 0 & 0 & 305 \end{bmatrix}[\mathrm{rad}^2].$$

The high value of the last element is due to backlash in the last joint. For S_θ, on the different lengths (a_i, d_i, Δx_j^d, Δy_j^d, Δz_j^d), $\sigma = 0.001$ m. On the different angles (α_i, β_i, $\Delta\phi_{xj}^d$, $\Delta\phi_{yj}^d$, $\Delta\phi_{zj}^d$), $\sigma = 3° = 0.052$ rad.

D. Remarks

Before presenting our results, we have to make some remarks and comments.

Nonuniqueness of the Solution: If we consider the global set of geometrical parameters one can point out that the orthogonality of different parameters is far from being guaranteed. Indeed, some parameters are not even independent. For example, an error on θ_1 has the same effect on the end-effector position as an error on the measuring device position and orientation. In a similar way, an error on d_2 or on d_3 has the same effect on the end-effector. Nonuniqueness of the solution is not a real problem considering the user's point of view. The obtained solution will guarantee a certain level of accuracy according to a least squares fit of the parameters. But, surprisingly, if the global geometrical model is satisfactory, the errors identified, taken one by one, do not have a real physical meaning. Furthermore, it can be shown that, in the Jacobian matrix, the columns associated with the geometrical parameters are far from being orthogonal to the ones associated with the nongeometrical errors. Therefore, if nongeometrical errors are not included in the estimation, their effects will be distributed over geometrical parameters, so that the attribution of estimated values to specific physical errors may be meaningless.

Fixed Parameters: Following the same idea, it is important to try to find some parameters that could not be identified. This can be done by carefully examining the robot kinematic structure. In our case we have decided to "freeze" the following geometrical parameters:

- θ_1 is an error on θ_1 has the same effect as some position and orientation error of the measuring device;
- α_6 is an error on α_6 is not observable;
- d_1 is an error on d_1 has the same effect as Δz_j^d, device position error in the vertical direction; and
- d_2 is an error on d_2 has the same effect as an error on d_3.

On the other hand, a twist error β_2 must be introduced, to take into account a nonexact parallelism between axes z_1 and x_2. Those two remarks are also presented in [1], [7], and [11].

E. Errors on Electrical Zeroes of Joint Encoders

Our first results are related to a case in which we only consider errors on the joint encoder zeroes; we consider $\Delta\theta_i \neq 0$ and $\Delta\alpha_i = \Delta d_i = \Delta a_i = \Delta\beta_i = 0$ for all i. As we know from [13] and [14], the joint angle offsets are by far the largest contributor to the end error (about 90%), so that a significant improvement of the geometrical model can be expected after identification. During the experimental work, we measured 12 points on each line, with a total of 5 lines in the workspace. One of those lines is only used for validation of the identification results. Before identification, the mean end-effector position error on the total set of measurements belonging to the first 4 lines is equal to $\bar{e} = 11.28$ mm. After a first run of the identification algorithm, the average error is equal to $\bar{e}_1 = 4.95$ mm.

To improve our results it is appropriate to use our first-order linearized model in a next iteration, as we said in Section II-C, taking the covariance matrix P_N of the previous run for P_0 of the next run, and the estimates $\hat{\theta}_N$ of the previous run for the initial guess $\hat{\theta}_0$ of the next run. After the second run the average error is equal to $\bar{e}_2 = 0.89$ mm. After the third run the average error is equal to: $\bar{e}_3 = 0.81$ mm. Further runs do not improve the solution.

Errors identified are as follows (in radians):

$$\Delta\theta_2 = 0.0236$$
$$\Delta\theta_3 = -0.1277$$
$$\Delta\theta_4 = -0.0341$$
$$\Delta\theta_5 = 0.2585$$
$$\Delta\theta_6 = -0.0109.$$

The square roots of the diagonal elements of the final covariance matrix are, respectively,

$$\sigma_2 = 0.0005 \text{ rad}$$
$$\sigma_3 = 0.0007 \text{ rad}$$
$$\sigma_4 = 0.0014 \text{ rad}$$
$$\sigma_5 = 0.0010 \text{ rad}$$
$$\sigma_6 = 0.0148 \text{ rad}.$$

On the validation line, we have a mean end-effector position error equal to $\bar{e}_v = 10.83$ mm before identification and $\bar{e}_{v3} = 0.81$ mm using the results of identification, which is very close to the results obtained for the identification lines.

F. User-Adjustable Geometrical Parameters on the Siemens Control Unit

As we already mentioned, the Siemens RCM-SIROTEC control unit that we use with our home made robot allows the user to adjust only a subset of the geometrical parameters. Therefore, we search for a set of values for the adjustable parameters that best fit the data included in the estimation process; we must keep in mind the fact that this set of geometrical values may be valid only in a limited area of the robot workspace.

In our case, we can adjust the angular offsets for θ_1, $\theta_2, \ldots, \theta_6$, and the link lengths a_2, a_6, d_4, d_6. The parameter θ_i, will not be adjusted (see remarks in Section III-D). We have used the same measurements as in Section III-E.

After the first run of the algorithm, the mean error is equal to $\bar{e}_1 = 3.15$ mm. After the 12th run, the mean error is equal to $\bar{e}_{12} = 0.61$ mm. More runs do not improve the solution.

Identification results are

$$\Delta\theta_2 = 0.0049 \text{ rad } (0.0002 \text{ rad})$$
$$\Delta\theta_3 = -0.0995 \text{ rad } (0.0005 \text{ rad})$$
$$\Delta\theta_4 = -0.0334 \text{ rad } (0.0010 \text{ rad})$$
$$\Delta\theta_5 = 0.1760 \text{ rad } (0.0012 \text{ rad})$$
$$\Delta\theta_6 = 0.3122 \text{ rad } (0.0122 \text{ rad})$$
$$\Delta a_2 = -0.0022 \text{ m } (0.00011 \text{ m})$$
$$\Delta d_4 = -0.0148 \text{ m } (0.00034 \text{ m})$$
$$\Delta a_6 = 0.0017 \text{ m } (0.00008 \text{ m})$$
$$\Delta d_6 = 0.0166 \text{ m } (0.00010 \text{ m}).$$

Values in parentheses are the square roots of the covariance matrix diagonal elements. On the validation line we have, using the results of the identification, a mean end-effector position error equal to $\bar{e}_{v12} = 0.68$ mm, which is of the same order as the mean error for the four identification lines.

G. Comments

1) The improvement achieved by taking into account Δa_2, Δd_4, Δa_6, and Δd_3 is about 25%.

2) The difference on some values of error between the two cases is significant.

	1st Case (rad)	2nd Case (rad)
$\Delta\theta_2$	0.0236	0.0049
$\Delta\theta_5$	0.2585	0.1760
$\Delta\theta_6$	−0.0109	0.3122

This fact clearly illustrates the difficulty of a physical interpretation of the identification results because of the noncompleteness of the model adopted

3) Experimental results clearly show that a lower bound exists on the calibration error that is dictated by robot repeatability and calibration accuracy. The latter depends in turn on the accuracy of the measurement system and the inaccuracies due to robot parameters that are not modeled (nongeometrical errors).

4) The choice of the measuring lines is dictated by two considerations. The first is that there exist some areas in the robot workspace where the position error is large. For calibration purposes, it is interesting to explore such regions that can be found by an *a priori* analysis (see Section II-D). The reason is that measurement errors become less significant. The second consideration is that the set of the geometrical values identified can be valid in a limited area of the robot workspace because an incomplete set of parameters has been adopted in the modeling process and no nongeometrical effects have been taken into account. This suggests that the measuring lines must be chosen in a restricted region of the workspace, particularly in the zones where the task must be performed with great accuracy.

5) We have compared the performances of the recursive maximum likelihood (ML) estimator, against the recursive least squares (LS) algorithm, by running the latter on the same measurement data set. The initial estimate of the covariance matrix $P(0)$ $(= P_0 I_n)$ was chosen such that convergence rate was optimal. Fig. 4 shows the module of the prediction error (see Section II-F for the definition) during the identification process.

Notice that:

a) Each measuring line involves 10 points. The first two points are used to compute an initial estimate of the position and the orientation of the line, so that 8 points are effectively used for identifications.

b) Each time that a new measuring line is taken up, the prediction error abruptly increases because several extra parameters (related to position and orientation error of the line) must be identified.

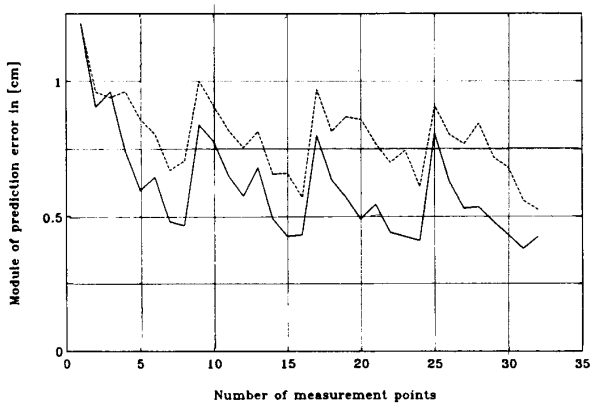

Fig. 4. Comparison of maximum likelihood and least squares algorithms convergence.

c) Prediction errors obtained by the ML algorithm are smaller and, after four lines have been explored, the accuracy of the estimation is better than with the LS algorithm. However, we observed that the accuracy levels become nearly identical if a large number of measurement points is used.

IV. Use of Improved Geometrical Model

The improved geometrical model obtained after identification of the geometrical parameter errors can be used in different ways.

A. Error Map

The error map is obtained by plotting, in a cross-section of the robot workspace, the end-effector position error vector norm, based on the knowledge of the nominal geometrical model and the improved model. We call the nominal position vector of the end effector x_n and the position vector of the end effector computed by using the identified geometrical parameters x_i. Both these terms are defined with respect to the robot frame. These quantities are functions of q_i:

$$x_n = f_n(q) \tag{29}$$

$$x_i = f_i(q) \tag{30}$$

where f_n is the nominal geometrical model and f_i is the improved geometrical model. The error vector norm is obtained by

$$e = \| x_i - x_n \| = \| f_i(q) - f_n(q) \|. \tag{31}$$

Plotting e as a function of the Cartesian coordinates in a workspace cross section gives us information on subspaces, showing which are more or less accurate than other ones (see Fig. 5 representing an error map in a vertical cross-section of our robot workspace). This information is very helpful for the design of the layout of a robot cell when the robot control system and the off-line programming system do not permit compensation for the end-effector errors by using the other methods here described. The idea of this error map is a continuation of the concept of a *a priori* analysis and *a posteriori* analysis of geometrical model errors presented in [7].

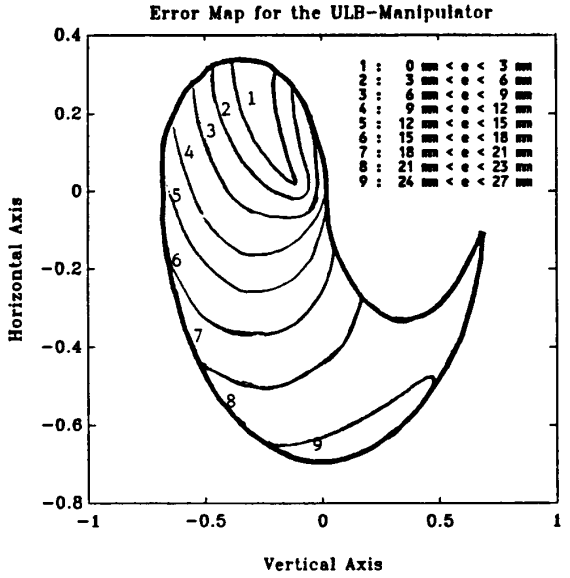

Fig. 5. Error map in a vertical cross section of the ULB manipulator workspace ($\theta_1 = \theta_4 = \theta_6 = 0$ – elbow up).

B. Action on the Target: Task Space Correction

If we cannot modify the geometrical model inside the robot control unit, but we can adapt the off-line programming system, then we may change the target in the task space in such a way that the end effector will reach the initial desired target x_d [9]: this is the "false target" technique.

Let us call the desired target x_d, the target reached by the end-effector without correction ($\neq x_d$): x_n, and the modified target x_m. With a very good approximation, x_m is given by

$$x_m = x_d + (x_d - x_n) = 2x_d - x_n$$
$$= 2x_d - f_i(f_n^{-1}(x_d)). \tag{32}$$

The modified target x_m is presented to the control unit, which computes

$$q_m = f_n^{-1}(x_m). \tag{33}$$

This type of algorithm requires to handle two inverse nominal models and one direct improved model. Similar algorithms are presented in [1] and [5], while [14] proposed an improved iterative version of this one.

C. Correction in the Joint Space

Obviously, the best way to use the improved geometrical model is to replace the inverse nominal geometrical model by the improved one in the robot control unit. But by doing so it is no longer possible to find an analytical solution for the inverse geometrical problem. Therefore, iterative methods (like the Newton–Raphson methods) must be implemented in the control unit in order to convert the Cartesian task into an articular one, using the improved geometrical model [2].

If the inverse geometrical model of the control unit cannot be improved directly, but we can control the robot directly in the joint variable space, then we can use the following

algorithm to compensate for the error [9]:

$$q_i = f_n^{-1}(x_d) + J_n^{-1}(x_d - x_n) = f_n^{-1}(x_d) + J_n^{-1}(x_d - f_i(f_n^{-1}(x_d)) \quad (34)$$

where J is the classical Jacobian matrix of the manipulator and q_i the input of the robot controller. This algorithm requires one inverse nominal model, one improved direct model, and one inverse Jacobian of the nominal model.

If the identification results show that the errors on the electrical zeroes of the encoders are responsible for the greatest part of the total end-effector error, and if the robot can be controlled in the joint space, we propose simply:

$$q_i = f_n^{-1}(x_d) - \Delta q \quad (35)$$

where q_i represents inputs of the robot controller and Δq represents identified angular offset errors. This technique only requires us to compute the inverse of the nominal model. Moreover, this computation can be performed off line.

V. Conclusions

The proposed method, including the algorithm and the measuring device, shows very good results in improving the accuracy of the robot model. In our opinion, an error of 0.5 mm must be considered as the best result that can be obtained without considering the nongeometrical errors. During our experiments, we have loaded the end-effector with a load of 1 kg: the resulting deflection was 0.2 mm. Furthermore, backlash introduces errors of the same order. These facts explain our figure of 0.5 mm. The algorithm does not consider only the errors that have to be identified but also the input and output noises. It presents a recursive form with a reasonable amount of computation. It offers the possibility of following the convergence rate and direction of the solution step by step and of detecting and eliminating possible faulty measurements. We have summarized the different ways to use the improved geometrical model. In the future, efforts should be focused on the nongeometrical errors with the aim of bringing the accuracy of the system close to the resolution of the encoders.

Acknowledgment

The authors would like to thank Dr. M. Kinnaert from the Free University of Brussels, N. Mitchison from the Joint Research Center of Ispra (Italy), and the reviewers for their helpful comments and suggestions.

References

[1] W. K. Veitschegger and C. H. Wu, "A method for calibrating and compensating robot kinematic errors," in *Proc. IEEE Int. Conf. Robotics Automat.* (Raleigh, NC), 1987, pp. 39-44.

[2] M. S. Cai and A. Rovetta, "Position and orientation error analysis and a contribution to Newton's method for solving the inverse kinematic for robot manipulator," in *Proc. Int. Conf. Comput. Intell.* 88 (Milan, Italy), 1988, pp. 211-220.

[3] J. M. Hollerbach and Bennett, "Automatic kinematic calibration using a motion tracking system," in *Robotics Res. 4th Int. Symp.* Cambridge, MA: MIT Press, 1988, pp. 191-198.

[4] C. H. An, C. G. Atkeson and J. M. Hollerbach, *Model-Based Control of a Robot Manipulator.* Cambridge, MA: MIT Press, 1988, ch. 3, pp. 49-64.

[5] A. Preumont, E. Ponslet, and D. Lefeber, "Improvement of the geometrical model of robot manipulators," presented at *Int. Symp.* ACD&D '89 Tokyo, Sept. 1989.

[6] B. C. Jiang, J. T. Black, and J. N. Hool, "Taguchi methods-based robot metrology," in *Proc. Robots 13 Conf.* (Gaithersburg, MD), May 1989, pp. 145-159.

[7] M. Becquet, J. M. Renders, and E. Ponslet, "Kinematic model sensitivity to geometricalal parameters errors and its impact on robotic precision," in *Proc. 3rd Int. Conf. CAD/CAM, Robotics and Factories of the Future* (Southfield), Aug. 1988.

[8] M. Becquet and D'Haemers, "Static and dynamic performance measurements of industrial robots," *Revue M,* vol. 32, no. 1/2, 1988.

[9] D. Payannet, M. J. Aldon, and A. Liégeois, "Identification and compensation of mechanical errors for industrial robots," in *Proc. 15th ISIR* (Tokyo), Sept. 1985, pp. 857-864.

[10] M. Ishii, S. Sakane, M. Kakikura, and Y. Mikami, "A new calibration system for improving absolute accuracy of robot manipulators," in *Proc. 16th ISIR,* 1986, pp. 1017-1025.

[11] J. Chen and L. M. Chao, "Position in error analysis for robot manipulators with all rotary joints," in *Proc. IEEE Int. Conf. Robotics Automat.* (San Francisco), 1986, pp. 1011-1016.

[12] M. Ishii, S. Sakane, and Y. Mikami, "A 3-D sensor system for teaching robot paths and environments," *Int. J. Robotics Res.,* vol. 6, no. 2, pp. 45-56, Summer 1987.

[13] D. E. Whitney, C. A. Lozinski, and J. M. Rourke, "Industrial robot forward calibration method and results," *ASME J. Dynamic Syst., Measurements Cont.,* vol. 108, pp. 1-8, Mar. 1986.

[14] R. P. Judd and A. B. Knasinski, "A technique to calibrate industrial robots with experimental verification," in *Proc. IEEE Int. Conf. Robotics Automat.* (Raleigh, NC), 1987, pp. 351-357.

[15] H. W. Stone and A. S. Sanderson, "A prototype arm signature identification system," in *Proc. IEEE, Int. Conf. Robotics Automat.* (Raleigh, NC), 1987, pp. 175-182.

[16] J. H. Gilby and G. A. Parker, "Laser tracking system to measure robot arm performance," *Sensor Rev.,* vol. 2, no. 4, pp. 180-184, 1982.

[17] M. Becquet, "Analysis of flexibility sources in robot structures," in *Proc. IMACS/IFAC Int. Symp. Modeling and Simulation of Distributed Parameter Syst.* (Hiroshima, Japan), 1987, pp. 419-424.

[18] W. K. Veitschegger and C. H. Wu, "Robot accuracy analysis based on kinematics," *IEEE J. Robotics Automat.,* vol. RA-2, pp. 171-180, Sept. 1986.

[19] L. Ljung, *System Identification – Theory for the User.* Englewood Cliffs, NJ: Prentice-Hall, 1987.

[20] C. H. Menq and J. H. Borm, "Statistical measure and characterization of robot errors," in *Proc. IEEE Int. Conf. Robotics Automat.,* 1988, pp. 926-930.

[21] Z. S. Roth, B. W. Mooring, and B. Ravani, "An overview of robot calibration," *IEEE J. Robotics Automat.,* vol. RA-3, no. 5, pp. 377-384, Oct. 1987.

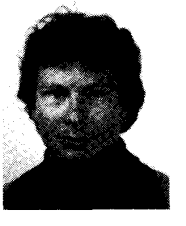

Jean-Michel Renders was born in Brussels, Belgium. He received the Master's degree in mechanical and electrical engineering from the University of Brussels, Brussels, Belgium, in 1987. He is currently working toward the Ph.D. degree at the Joint Research Center of the European Communities at Ispra, Italy. His research interests include adaptative learning control of robotic manipulators, nonlinear control theory, and application of biological adaptive mechanisms (including neural and immune networks) to process control.

Eric Rossignol was born in Brussels, Belgium, in 1964. He graduated with a degree in electrical and mechanical engineering in 1987 from the University of Brussels.

He joined the research team ARC Robotique (PRAGMA) at the University of Brussels in 1987. His main research subject is the amelioration of the dynamical performances of manipulation robots and instrumentation. He is preparing a thesis on hybrid control position force.

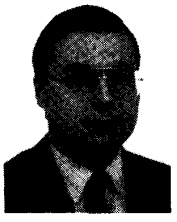

Marc Becquet was born in Antwerpen, Belgium. He received the Master's degree in electromechanical engineering and the Ph.D. degree from the University of Brussels (ULB), Brussels, Belgium, in 1983 and 1987, respectively.

From 1987 to 1989, he was a Project Manager in Robotics at ULB. He is now a Scientific Officer at the Institute of Systems Engineering and Informatics, Joint Research Center, Commission of the European Communities, where he is in charge of the Telemac Laboratory. His research interests include robotics, remote handling for thermonuclear fusion devices like JET and NET/ITER, and computer aided design. He is also an Associate Professor at the Solvay Business School, University of Brussels.

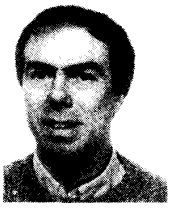

Raymond Hanus received degrees in physical engineering and in automatic control engineering from the University of Brussels (ULB), Brussels, Belgium, in 1970 and 1972, respectively. He received the Doctorate in Applied Sciences from the University of Brussels in 1979.

He is currently Professor of Automatic Control and Director of the Control Engineering Department of ULB. His main research interests are in the identification and control of nonlinear systems.